Electrochemistry Communications 162 (2024) 107700

Contents lists available at ScienceDirect

Electrochemistry Communications

journal homepage: www.elsevier.com/locate/elecom

Suppression of dendrite formation via ultrasonic stimulation

Yifeng Zhang [a,1], Haobo Dong [b,1], Ruoxi Yang [a], Hongzhen He [b], Guanjie He [c], Frederic Cegla [a,*]

[a] NDE Group, Department of Mechanical Engineering, Imperial College London, South Kensington Campus, London SW7 2AZ, UK
[b] Electrochemical Innovation Lab, Department of Chemical Engineering, University College London, Torrington Place, London WC1E 7JE, UK
[c] Department of Chemistry, University College London, 20 Gordon Street, London WC1H 0AJ, UK

ARTICLE INFO

Keywords:
Battery
Ultrasonic stimulation
Acoustic streaming
Dendrite suppression

ABSTRACT

This research introduces a chemistry-agnostic approach to achieve rapid and degradation-free battery charging via ultrasonic agitation. An ultrasonic device operating in the megahertz range was used to stimulate electrolyte flow from outside the cell. The acoustic streaming effect accelerates ion transport from the bulk electrolyte to the electrode surface and suppresses the formation of an ion depletion zone. An experimental setup was used to optically observe the formation of dendrites when the current imposed across two zinc electrodes exceeded the limiting current. Beyond this limit, diffusion alone cannot provide sufficient ions, resulting in an ion depletion zone. It was subsequently shown that dendrite formation was reduced by over 98% when 15x the limiting current was forced across the electrodes and acoustic stimulation was delivered. Furthermore, it was shown that compared to the scenario without ultrasonic stimulation, the steady state potential was also reduced by 29%, indicating much better ion exchange between the electrodes. These findings suggest that ultrasonic stimulation can be a tool for enhancing electrochemical processes such as battery charging and discharging.

1. Introduction

The swift and degradation-free charging of batteries is a highly desirable characteristic and focal point of extensive research. However, most metallic battery systems today (e.g. lithium-ion batteries, zinc-ion batteries etc.) are still plagued by the issue of dendrite formation under high charging rate. Dendrites are protrusions resembling tree branches that develop on electrode surfaces during battery charging. They represent a prevalent battery degradation mechanism that can lead to reduced battery capacity and serious safety hazards such as short circuits and thermal runaway events.

In an aqueous zinc ion battery system, the charging process involves the reduction of electrolyte-borne Zn^{2+} and their deposition onto the anode surface. When battery electrolyte is stagnant (Fig. 1 (a)), ion transport from the bulk electrolyte to the electrode surface is driven by the diffusion process. Tip-growing dendrite growth is triggered when the charging current exceeds the diffusion limit as this creates a zone of cation depletion near the electrode that prevents uniform zinc deposition [1,2].

Considerable research efforts have been dedicated to mitigating or preventing the risk of dendrite formation. These approaches encompass exploring (a) alternative electrolyte composition [3], (b) addition of electrolyte additives [4], (c) surface modifications [5], (d) adoption of tailored charge/discharge protocol [6] etc. While many of these strategies have shown promising results, they are often tai- lored to certain chemical compositions and lack broad applicability across different battery systems (e.g., Li/Zn/Na batteries). An alternative,'chemistry-agnostic' approach to dendrite formation involves enhancing ion transport from the bulk electrolyte to the electrode surface, thereby averting the creation of a depletion zone near the electrode (Fig. 1 (b)).

Wang et al.[7] demonstrated that dendrite growth is controlled by the process of ion diffusion and can be suppressed by inducing electrolyte flow. Ma et al.[8] investigated the efficacy of cross-flow at different flow rates. The authors attributed its dendrite-suppressing effects to enhanced ion transport rate, caused by thinner ion concentration polarization zone and additional mechanism induced by convective flow. The authors also found that at high flow rate, convective flow overtook diffusion to become the dominating ion transport and replenishment mechanism.

To initiate the flow of electrolyte within a battery cell, current approaches primarily rely on mechanical means such as the use of syringe-like pumps [8], which are usually bulky and difficult to integrate into

* Corresponding author.
E-mail address: f.cegla@imperial.ac.uk (F. Cegla).
[1] Yifeng Zhang and Haobo Dong have equal contribution in this work.

https://doi.org/10.1016/j.elecom.2024.107700
Received 14 February 2024; Received in revised form 28 February 2024; Accepted 7 March 2024
Available online 11 March 2024

battery packs. Alternatively, the use of acoustic stimulation presents a potential alternative solution for inducing electrolyte flowing and mixing. Acoustic streaming occurs when the fluid is forced to oscillate in large amplitude such that the oscillation velocity exceeds the speed of sound in the fluid. In these cases, energy of the acoustic wave is partially absorbed by the fluid which results in a time-independent velocity component of the fluid. This phenomenon has been utilised extensively in biomedical applications for fluid mixing and drug delivery. For further details on the origin and modelling of acoustic streaming phenomena, readers are directed to literature such as [9,10,11].

Micro-streaming can arise from the implosion of cavitation bubbles when a fluid is subjected to low-frequency excitation. Doche et al [12] explored the influence of ultrasonic agitation on zinc corrosion and oxidation mechanism in a sodium sulfate electrolyte. Their study revealed that ultrasonic excitation at 20–40 kHz range greatly accelerates the rate of zinc oxidation and corrosion by enhancing mass transfer close to the electrode. Huang et al. [13] employed the ultrasonic capillary effect to induce electrolyte movement in an Aluminium-air flow cell. Via ultrasonic agitation at 40 kHz, the authors observed increased peak power density and short-circuit current density during sonification. Ultrasonic excitation at very high frequencies was employed in a series of studies by Huang et al. [14,15]. The authors embedded a surface acoustic waves (SAW) device into battery cells operating at 100 MHz frequency range. The SAW device was demonstrated to generate acoustic streaming and mitigate dendrite formation in cycled Li-ion batteries.

However, existing research are not without limitations. For instance, the cavitation effect resulted from low-frequency (20–40 kHz) ultrasonic agitation is known to induce extreme heat and can therefore damage the electrodes[16]. At the other end of the frequency spectrum, SAW devices operating at very high frequencies (100 MHz) often bear limited range and are challenging to scale up [11].

This study introduces an alternative ultrasound-based approach which operates in the megahertz frequency range. Compared to low-frequency excitation, the selected frequency range reduces the probability of cavitation and ion mixing predominantly arises from acoustic streaming. The generated ultrasonic wave has a wavelength in the order of (sub-)millimetre which enables better direction of the ultrasonic energy. Unlike the embedded high-frequency device, the megahertz frequency transducer can be externally installed on a cell. It was demonstrated in this study that the megahertz device can improve the electrochemical characteristics of the redox reaction and effectively suppressing dendrite formation on battery electrodes.

2. Methodology

Fig. 2 shows the schematic experimental arrangement for this study. A symmetric two-electrode assembly was placed in a transparent, cubic reaction vessel. A 3D printed fixture was used to control the immersion area of the electrode and the inter-electrode distance. In this study the immersion area was 1.5 cm^2 and the inter-electrode separation was 2 mm. An in-house built ultrasonic transducer (25 mm diameter, 1.6 MHz operating frequency) was placed underneath the reaction vessel for generating acoustic streaming effects inside the reaction vessel. The distance between the transducer and the top of the immersed area of the electrode was 4 cm (including a glass layer of 2 mm). The experimental setup and procedures are explained in more detail in Supplementary Information.

To demonstrate and assess the efficacy of the proposed ultrasonic agitation system, a DC current of 9.72 mA was applied to the symmetric cell to simulate a scenario of high- current charging processes. The imposed current density was approximately 15 times greater than the diffusion-controlled limiting current density J_{lim} which can be estimated using Equation (1) [1]. The choice of such a high current density ensures that the system operates under an over-limiting- current condition and tip-growing dendrite growth can be induced on the electrode surface.

$$J_{lim} = \frac{2z_c F DC_0}{t_a L} = 0.433 mA/cm^2 \quad (1)$$

where $z_c = 2$ is the charge number of the zinc ion, $c_0 = 0.02M$ is the bulk electrolyte concentration, $F = 96{,}485$ is Faraday's Constant, $L = 2mm$ is the electrode separation distance. The value of Zn^{2+} ion diffusivity, D, is assumed to be $7 \times 10^{-10} m^2/s$ based on inference from relevant literature [17]. The transference number of the Zn^{2+} ion and the anion in the aqueous electrolyte are estimated to be $t_{Zn} = 0.376$ and $t_a = 1 - t_{Zn} = 0.624$, respectively [18].

The duration of each experiment was set to 300 s. The experiment was first run on a control setup with stagnant electrolyte (without ultrasonic agitation). During the experiment, the potential difference between the two electrodes was measured by the electrochemical working station at a rate of 10 measurements per second. Temperature measurements and optical images were acquired at every second. For the experiments with ultrasonic agitations, alternative peak-to-peak voltages (Vpp) of 25Vpp, 30Vpp, and 35Vpp were supplied to the ultrasonic transducer which correspond to an average power consumption of 6 W, 8 W and 11 W, respectively. All measurements in each experiment were synchronised in post-processing.

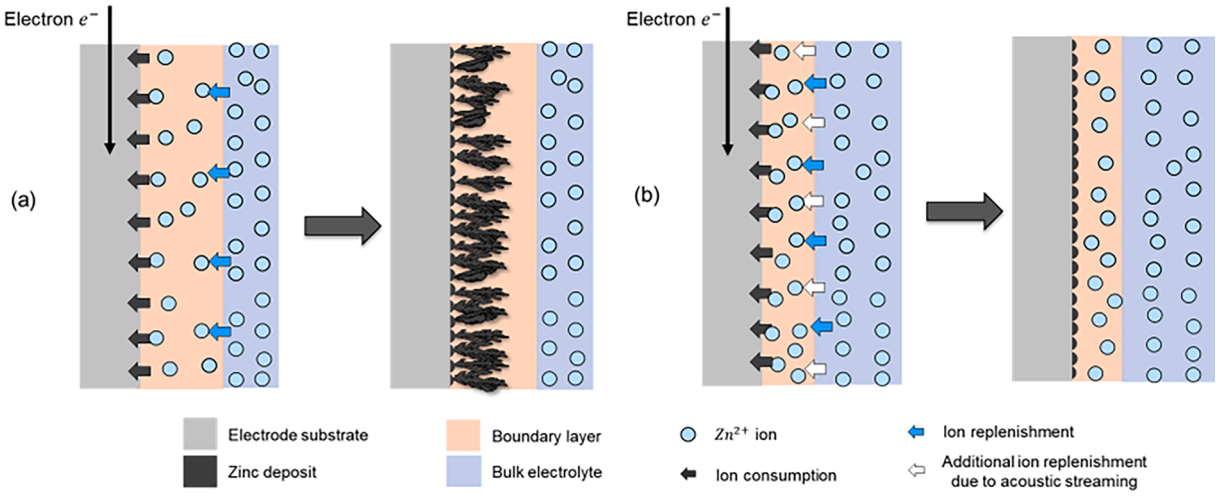

Fig. 1. (a) Without ultrasonic stimulation, charging above the diffusion-limiting rate leads to dendritic deposition. (b) With ultrasonic stimulation, acoustic streaming generates additional ion replenishing mechanism and ensures uniform deposition under over-limiting conditions.

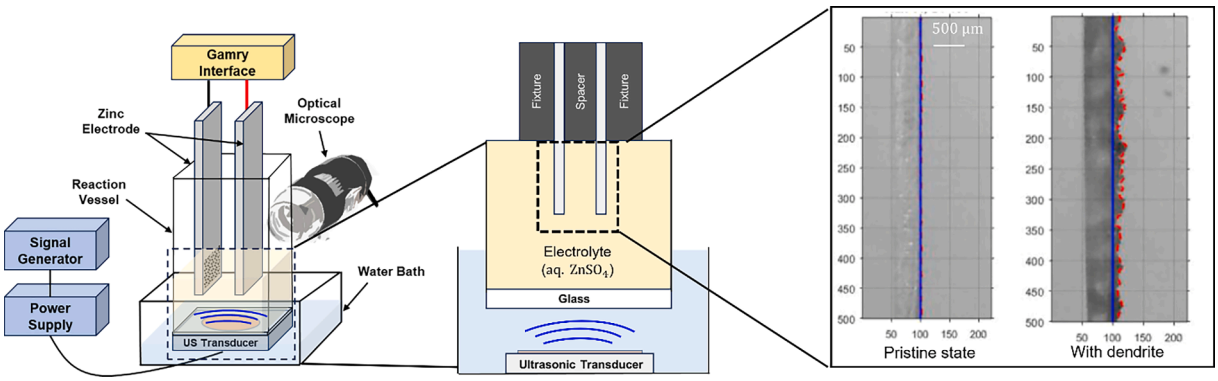

Fig. 2. Schematic sketch of the reaction vessel and experimental setup. Inset: example optical images of a pristine electrode and electrode with Zn dendrite.

3. Results and discussion

The surface evolution of the electrode undergoing zinc deposition is displayed in Fig. 3 (a). In the absence of ultrasonic agitation (i.e. when the electrolyte is stagnant), black zinc deposit can be observed in the image acquired at 30 s after the onset of DC current. The thickness of the dendrite layer continued to grow over time afterwards and exceeded 775 um by the end of the experiment. The temporal evolution of dendrite height inferred from these images is plotted in Fig. 4 (b) and the rate of dendrite growth is shown in Fig. 4 (c). Note that a 5-point, leading-window moving average filter has been applied to the growth rate estimate to mitigate the effect of measurement noise. A time lapse video clip showing synchronized electrochemical measurements, in- situ optical images and dendrite height estimate is presented in the Supplementary Information (SI). Post-experiment, ex-situ optical and scanning electron microscope (SEM) images displayed in Fig. 3 (c) and (d) show clusters of loose, branch-like zinc deposit. In contrast, under the influence of ultrasonic stimulation (V = 35Vpp), the thickness of the plated layer was nearly indistinguishable in the in-situ the optical images. Ex-situ optical and SEM images in Fig. 3 (e) and (f) show clusters of compact and spherical zinc deposit uniformly distributed on the electrode surface, contrasting with the dendritic deposit observed in the earlier case. Ex- situ X-Ray diffraction (XRD) analysis (Figure S1, Table S1) measured a 6-time increase (0.026 to 0.168) in normalized intensity ratio [19] for the Zn (002) crystal plane, suggesting that the Zn (002) crystal plane was preferably formed under the influence of the imposed acoustic stimulation.

Electrochemical measurements further prove this dendrite inhibiting mechanism. Fig. 4 (a) shows the potential variation under a constant charging current (15× J_{lim}). Without ultrasonic stimulation, the electrical potential shows an overshoot of 900 mV shortly after the start of the charging process. In contrast, the magnitude of potential overshoot was reduced to 710 mV when the cell was stimulated by an external ultrasonic source of 25Vpp. The existence of potential overshoot can be attributed to cation depletion within the space-charge-layer (SCL) close to the electrode surface. From the perspective of diffusion dynamics and

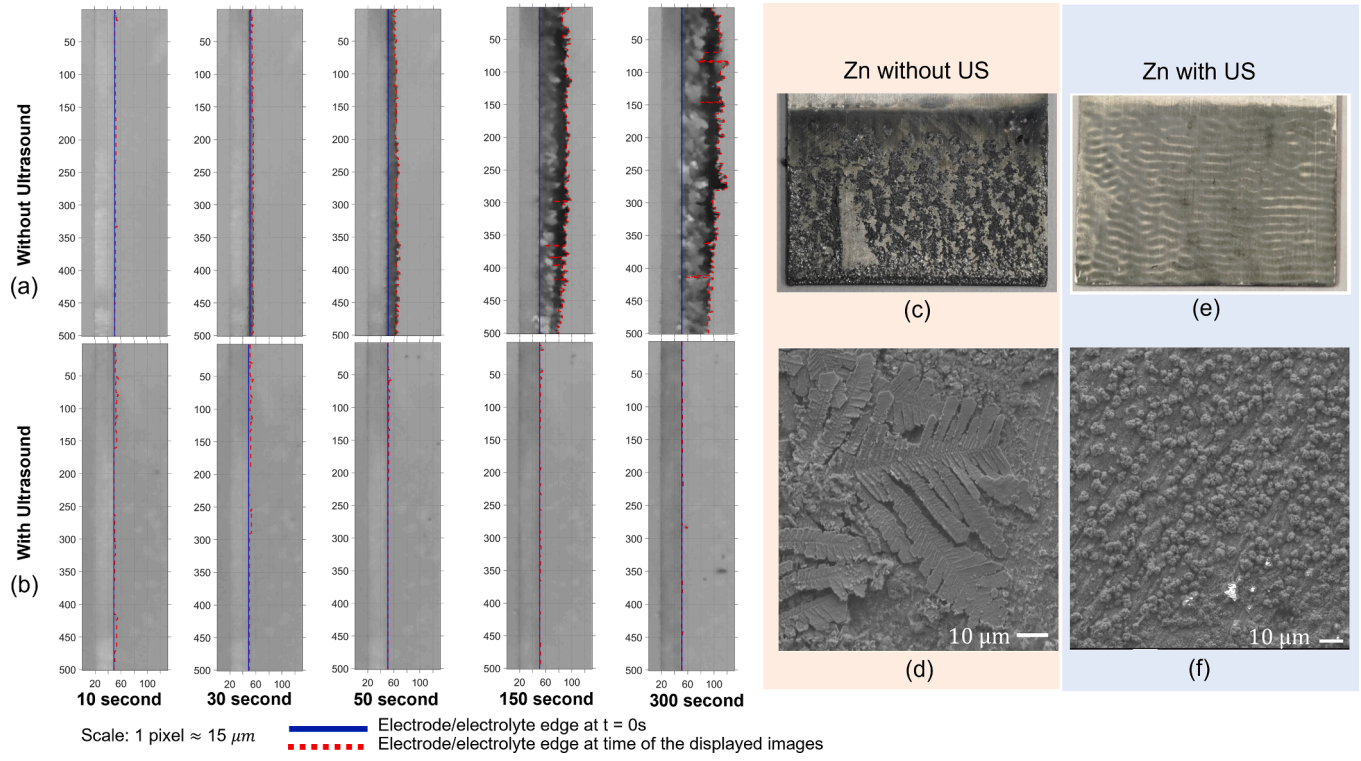

Fig. 3. In-situ optical images acquired at the displayed times (a) without, and (b) with ultrasonic stimulation. Ex-situ optical and SEM images of the electrode surface (c-d) without and (e-f) with ultrasonic stimulation (V = 35Vpp).

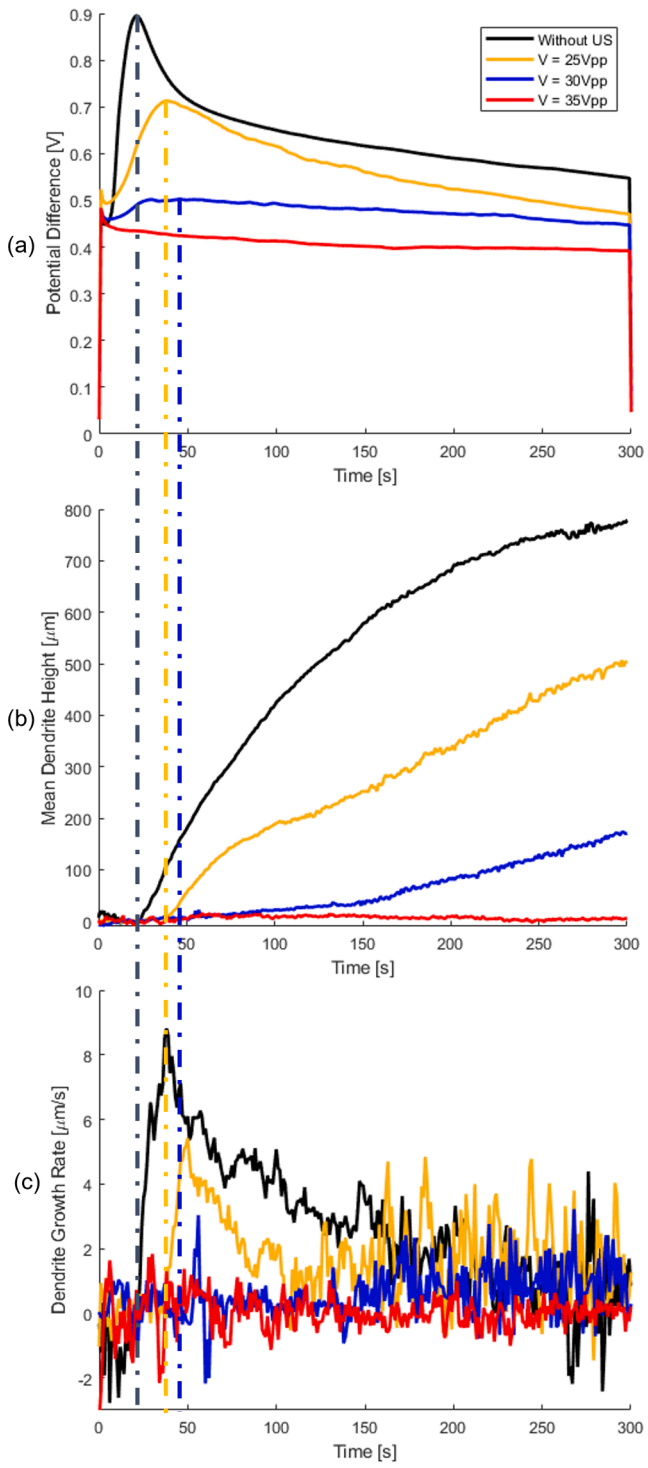

Fig. 4. (a) Potential difference variations between electrodes over time. (b) Temporal evolution of dendrite height. (c) Variation of dendrite growth rate over time. A 5-point, leading- window moving average filter is applied to the growth rate estimate to mitigate the effect of measurement noise.

thermodynamics, the reduction in overpotential implies increased number of active nucleation sites and more energetically favorable nucleation process, promoting uniform and controlled deposition [20,21] Previous study [8] suggested that the formation of depletion zone triggers electroconvective instabilities and generates chaotic electroconvective vortices. These vortices circulate cations to the electrode surface but also disrupt ion concentration gradients, promoting three-dimensional dendrite growth and ramifications. Our experimental observation corroborates with this theory. Without ultrasonic stimulation, the electrical potential rises in the first 20 s but the deposited zinc layer was unnoticeable on synchronized in-situ optical measurements in Fig. 4 (b) and (c); however, rapid, tip-growing dendritic deposition was immediately observed once the overpotential reaches its peak and starts to drop, suggesting the onset of vortex induced ion replenishment. In contrast, with ultrasonic stimulation, the onset of dendritic deposition is delayed from t = 21 s to 38 s. This implies a postponed formation of depletion zone under constant ion consumption rate, indicating that the acoustic streaming effect enhances the rate of ion migration and promotes two-dimensional, (002) plane rich depositions.

The study subsequently explored the efficacy of various levels of acoustic streaming in suppressing dendrite formation. The voltage supplied to the ultrasonic transducer was incrementally raised from 25 Vpp to 30 Vpp and then to 35 Vpp. It was visually confirmed during the experiments that the induced fluid motion aligns with the magnitude of excitation power. As illustrated in Fig. 4, increasing acoustic streaming effects result in further reduction in potential overshoot and further delay in dendritic deposition. In the case of V = 35Vpp, potential overshoot is completely eliminated, suggesting the absence of a depletion zone even under a very aggressive charging rate ($15\times J_{lim}$). This is supported by synchronized in-situ optical images that reveal negligible dendrite growth, i.e < 15 μm, or > 98 % reduction in terms of average dendrite height. The steady state electrical potential at the end of the charging period was also significantly reduced by 29 % from 550 mV to 390 mV, indicating a smaller internal resistance.

The current investigation serves as an initial exploration into dendrite suppression via external ultrasonic stimulation. Due to the intricate nature of acoustic streaming, an in-depth characterization of the induced flow patterns and flow rates necessitates sophisticated measurements that exceed the scope of this study. For instance, as shown in Fig. 3(e), a pattern of alternating strips can be observed on the surface of the electrode subjected to ultrasonic stimulation. Its spatial periodicity corresponds to half of the ultrasonic wavelength and is believed to be caused by a standing wave that forms between the electrodes. The standing wave affects the acoustic streaming pattern and hence influences the local mixing of ions. The pattern can be alternated or mitigated by adopting frequency sweeps and modulations which will be one of the future work. As such, significant improvements in its energy efficiency may be obtained through design optimisations such as transducer selection and placement. A deeper understanding of the ion replenishment mechanisms induced by the acoustic streaming effect is imperative in the design optimization. Therefore, comprehensive experimental and numerical studies that relate acoustic fields, electrolyte movement and electrochemical reactions are recommended as future work to transform this concept into practical engineering applications. Significant benefits, including extended battery longevity and applications in scenarios requiring very high charging rates, could be realized, thereby enhancing battery performance and safety.

4. Conclusion

This investigation introduces an ultrasound-based, chemistry-agnostic technique aimed at inhibiting dendrite formation, a common issue in metallic batteries that hinders their applications at high charging rate. A megahertz-rate ultrasonic device was employed to induce electrolyte flow via the acoustic streaming effect from outside a zinc battery cell. Ultrasonic stimulation was shown to delay or even prevent the formation of the depletion zone near electrodes, thus promoting uniform deposition even at over-limiting current conditions. Continuous, synchronized in-situ optical measurements demonstrated a correlation between dendrite formation and electrical potential, aligning with previous research findings. At an input power of 11 W, dendrite height under an aggressive charging rate (15 × the diffusion-limited current) was reduced by over 98 %, and the steady-state potential exhibited a 29 % decrease. Given its potential to enhance battery safety

and performance, further exploration of the topic is recommended, and directions for future research are outlined.

CRediT authorship contribution statement

Yifeng Zhang: Writing – original draft, Methodology, Investigation, Funding acquisition, Formal analysis, Conceptualization. **Haobo Dong:** Writing – original draft, Formal analysis. **Ruoxi Yang:** Investigation, Formal analysis. **Hongzhen He:** Investigation. **Guanjie He:** Writing – review & editing. **Frederic Cegla:** Writing – review & editing, Methodology, Funding acquisition, Formal analysis, Conceptualization.

Declaration of competing interest

The authors declare that they have no known competing financial interests or personal relationships that could have appeared to influence the work reported in this paper.

Data availability

Data will be made available on request.

Acknowledgement

Yifeng Zhang and Frederic Cegla would like to acknowledge the UK Acoustic Network Plus (UKAN+) for funding support [EP/V007866/1]. Haobo Dong would like to acknowledge the support via the UK Science and Technology Facilities Council Early Research Award [ST/R006873/1]. The authors would like to thank Mr Antonio De Sanctis in the Department of Mechanical Engineering at Imperial College London for his support in manufacturing the test rig.

Appendix A. Supplementary data

Supplementary data to this article can be found online at https://doi.org/10.1016/j.elecom.2024.107700.

References

[1] Peng Bai, Ju Li, Fikile R. Brushett, Martin Z. Bazant, Transition of lithium growth mechanisms in liquid electrolytes, Energ. Environ. Sci. 9 (10) (2016) 3221–3229.
[2] J. Eaves-Rathert, K. Moyer, M. Zohair, C.L. Pint, Kinetic- versus diffusion-driven three-dimensional growth in magnesium metal battery anodes, Joule 4 (6) (2020) 1324–1336.
[3] G. Bieker, M. Winter, P. Bieker, Electrochemical in situ investigations of SEI and dendrite formation on the lithium metal anode, PCCP 17 (14) (2015) 8670–8679.
[4] W. Zhang, Y. Dai, R. Chen, Xu. Zhenming, J. Li, W. Zong, H. Li, Z. Li, Z. Zhang, J. Zhu, F. Guo, X. Gao, Du. Zijuan, J. Chen, T. Wang, G. He, I. Parkin, Highly reversible zinc metal anode in a dilute aqueous electrolyte enabled by a pH buffer additive, Angew. Chem. Int. Ed. (2022) 210016.
[5] J.H. Han, E. Khoo, P. Bai, M.Z. Bazant, Over- limiting current and control of dendritic growth by surface conduction in nanopores, Sci. Rep. 4 (2014) 1–8.
[6] Z. Hou, Y. Gao, R. Zhou, B. Zhang, Unraveling the rate- dependent stability of metal anodes and its implication in designing cycling protocol, Adv. Funct. Mater. 32 (7) (2022) 1–8.
[7] Keliang Wang, Pucheng Pei, Ze Ma, Huicui Chen, Huachi Xu, Dong- fang Chen, Xizhong Wang, Dendrite growth in the recharging process of zinc-air batteries, J. Mater. Chem. A 3 (45) (2015) 22648–22655.
[8] M.C. Ma, G. Li, X. Chen, L.A. Archer, J. Wan, Suppression of dendrite growth by cross-flow in microflu- idics, Sci. Adv. 7 (8) (2021) 1–9.
[9] Wu. Junru, Acoustic streaming and its applications, Fluids 3 (4) (2018).
[10] Jeffrey S. Marshall, Junru Wu, Acoustic streaming, fluid mixing, and particle transport by a gaussian ultrasound beam in a cylindrical container, Phys. Fluids 27 (10) (2015).
[11] L.Y. Yeo, J.R. Friend, Surface acoustic wave microflu- idics, Annu. Rev. Fluid Mech. 46 (2014) 379–406.
[12] M.L. Doche, J.Y. Hihn, A. Mandroyan, R. Viennet, F. Touyeras, Influence of ultrasound power and frequency upon corrosion kinetics of zinc in saline media, In *Ultrasonics Sonochemistry* 10 (2003) 357–362.
[13] H. Huang, P. Liu, Q. Ma, Z. Tang, M. Wang, J. Hu, Enabling a high-performance saltwater al-air battery via ultrasonically driven electrolyte flow, Ultrason. Sonochem. 88 (July) (2022).
[14] A.n. Huang, H. Liu, O. Manor, P. Liu, J. Friend, Enabling rapid Charging lithium metal batteries via Surface acous- tic wave-driven electrolyte flow, Adv. Mater. 32 (14) (2020) 1–7.
[15] A.n. Huang, H. Liu, P. Liu, J. Friend, Overcoming the intrinsic limitations of fast charging lithium-ion batteries us- ing integrated acoustic streaming, Advanced Energy and Sustain- Ability Research (2022) 2200112.
[16] J. Klima, Application of ultrasound in electrochemistry. an overview of mechanisms and design of experimental arrangement, Ultrasonics 51 (2) (2011) 202–209.
[17] Y. Awakura, T. Doi, H. Majima, Determinatio of the diffusion coefficients of, Metallurgical and Materials Trans- Actions B 19 (February) (1988).
[18] J.L. Dye, M. Patricia Faber, D.J. Karl, Additions and corrections-transference numbers and conductances of multivalent salts in aqueous solution: zinc sulfate and zinc perchlorate, J. Am. Chem. Soc. 83 (24) (1961) 5047.
[19] G.B. Harris, Quantitative measurement of preferred orientation in rolled uranium bars, The London, Edinburgh, and Dublin Philosoph- Ical Magazine and Journal of Science 43 (336) (1952) 113–123.
[20] Haobo Dong, Xueying Hu, Ruirui Liu, Mengzheng Ouyang, Hongzhen He, Tianlei Wang, Xuan Gao, Yuhang Dai, Wei Zhang, Yiyang Liu, Yongquan Zhou, Dan J.L. Brett, Ivan P Parkin, Paul R Shearing, and Guanjie He. Bio-Inspired Polyanionic Electrolytes for Highly Stable Zinc-Ion Batteries. *Angewandte Chemie - International Edition*, 62(41), 2023.
[21] Yuhang Dai, Chengyi Zhang, Wei Zhang, Lianmeng Cui, Chumei Ye, Xufeng Hong, Jinghao Li, Ruwei Chen, Wei Zong, Xuan Gao, Jiexin Zhu, Peie Jiang, Qinyou An, Dan J.L. Brett, Ivan P. Parkin, Guanjie He, and Liqiang Mai. Reversible Zn Metal Anodes Enabled by Trace Amounts of Underpotential Deposition Initiators. *Angewandte Chemie - International Edition*, 62(18), 2023.